ELSEVIER

Coordination Chemistry Reviews
219–221 (2001) 81–97

COORDINATION CHEMISTRY REVIEWS

www.elsevier.com/locate/ccr

Coupled electron-transfer and spin-exchange reactions

Jeffrey W. Turner [1], Franklin A. Schultz *

Department of Chemistry, Indiana University Purdue University Indianapolis, 402 North Blackford Street, Indianapolis, IN 46202-3274 USA

Received 11 September 2000; received in revised form 5 December 2000; accepted 19 December 2000

Contents

Abstract

Electron-transfers accompanied by a change in metal atom spin-state occur widely in chemistry and biology. An appropriate framework for interpreting such behavior is an electrochemical scheme of squares consisting of two one-electron electrode reactions and two spin-equilibrium steps. The presence of coupled electron-transfers and spin-exchanges is reflected in the thermodynamic and kinetic parameters of such events. Oxidation–reduction potentials and electron-transfer rate constants depend on the positions of the spin-state

* Corresponding author. Tel.: +1-317-2782027; fax: +1-317-2744701.
E-mail address: schultz@chem.iupui.edu (F.A. Schultz).
[1] Present address: National Renewable Energy Laboratory, Mail Stop 3313, 1617 Cole Boulevard, Golden, CO 80401, USA.

PII: S0010-8545(01)00322-8

equilibria in the two oxidation states. Electrochemical activation parameters exhibit significant contributions from the large enthalpic and entropic differences that characterize spin-exchange reactions. The entropy of an electrochemical half-reaction, ΔS°_{rc}, coupled to a spin-exchange reflects the increases in vibrational and electronic entropy that accompany low- to high-spin conversion. Electrochemical enthalpies and entropies of activation, $\Delta H^{\ddagger}$ and $\Delta S^{\ddagger}$, are influenced by the temperature dependence of the accompanying spin-state transitions and are useful in mechanism diagnosis. The present review describes examples from the literature and our own laboratory regarding Fe(III/II) (d^5/d^6) and Co(III/II) (d^6/d^7) couples that exhibit the above behavior.

Keywords: Electron-transfer; Spin-exchange; Thermodynamic parameters; Kinetic parameters

1. Introduction

Reactions in which an electron-transfer is accompanied by a change in metal atom spin-state are widespread in chemistry and biology. Such processes are of interest because they are capable of regulating biological function [1–4] and of initiating molecular device operation [5–7]. A prominent example involves cytochrome P450, wherein substrate binding produces a change in the spin-state of the Fe(III) heme active site that shifts its redox potential, triggers an electron-transfer and initiates the catalytic cycle of the enzyme [8,9]. Other biological instances of coupled electron-transfer and spin-exchange occur in the iron–molybdenum cofactor of nitrogenase [10,11] and in cytochrome *c* peroxidases [12]. $Co^{3+/2+}$ self-exchange reactions [13] in which a low-spin Co(III) (t_{2g}^6) is reduced to a high-spin Co(II) ($t_{2g}^5e_g^2$) are familiar to coordination chemists. Although the issue has been debated for many years [14–21], it is still uncertain whether these reactions occur in a concerted manner between $S = 0$ and 3/2 ground states or involve high energy spin-states of Co^{3+} and/or Co^{2+} as intermediates.

Recent reviews [22–26] have described various aspects of spin-crossover behavior. However, reactions in which a spin-exchange is accompanied by a change in oxidation state have not received much attention. Our interest in the problem derives from efforts to understand the influence of inner-shell structure on electron-transfer reactivity. In the course of this work we investigated the electrochemistry of various metal-bis(1,4,7-triazacyclononane) (tacn) complexes [27] and found that $M(tacn)_2^{3+/2+}$ half-reactions characterized by a change in spin-state exhibited unusual activation parameters, although otherwise displaying structure–reactivity patterns in accord with the Marcus theory. This finding has led us to seek an explanation for this observation and to better understand the characteristics of coupled electron-transfer and spin-exchange reactions. The present article reviews the thermodynamics and kinetics of electrochemical reactions that are accompanied by a change in spin-state and illustrates the consequences of this behavior on the redox properties of coordination compounds.

2. Properties of spin-state reactions

2.1. Thermodynamics

Octahedral complexes of first-row transition elements with d^4 through d^7 configurations exhibit spin-state isomerism. Low-spin (ls) forms are favored by strong ligand fields and high-spin (hs) forms are favored by weak ones. However, at a range of ligand field strengths of intermediate value (dependent on metal atom and oxidation state), low- and high-spin configurations become sufficiently close in energy for both to be populated thermally at experimentally accessible temperatures. In solution, this results in a gradual, temperature dependent distribution between two species, as illustrated below for low- and high-spin iron(II).

$$\mathrm{ls-Fe(II)}[^1\mathrm{A}_1, t_{2g}^6] \rightleftharpoons \mathrm{hs-Fe(II)}[^5\mathrm{T}_2, t_{2g}^4 e_g^2] \quad K_{se} \tag{1}$$

$$K_{se} = [\mathrm{hs}]/[\mathrm{ls}] = \exp[\Delta S^\circ_{se}/\mathrm{R}] \exp[-\Delta H^\circ_{se}/\mathrm{R}T] \tag{2}$$

Reaction (1) is a chemical equilibrium. It is characterized by the spin-equilibrium constant, K_{se}, and the corresponding enthalpy and entropy of spin-exchange, ΔH°_{se} and ΔS°_{se}. These thermodynamic parameters can be determined from temperature dependent measurements that make use of the difference in magnetic and spectroscopic properties between low- and high-spin forms. Characteristically, ΔH°_{se} and ΔS°_{se} are positive quantities; thus, Reaction (1) is an entropically driven process in which the mole fraction of the hs form increases with increasing temperature. Spin-crossover is accompanied by significant nuclear reorganization. This occurs, because ls → hs conversion increases the occupancy of the σ-antibonding e_g orbitals, which lengthens and weakens the metal–ligand bonds. In addition, there is an increase in multiplicity associated with the electronic state change. These combined nuclear and electronic factors constitute the principal molecular contributions to ΔH°_{se} and ΔS°_{se}.

Table 1 contains structural, thermodynamic and kinetic data for a number of spin-exchange reactions [28–51]. The majority of examples involve Fe(II), but some Fe(III), Co(II) and Co(III) spin-equilibria have been studied. Most of the entries are characterized by a range of values, which reflects the extent to which solvent and, in some cases, counter ions influence ΔH°_{se}, ΔS°_{se}, $k_{ls\rightarrow hs}$ and $k_{hs\rightarrow ls}$. Although such environmental effects invariably are present, *in solution* they are small in comparison with the intramolecular factors described above and with large matrix effects that are frequently observed in solid phases. The positive values of ΔH°_{se} arise from the increase in metal–ligand bond distance (Δr) that accompanies the electronic state change and destabilizes the high-spin form of the complex. From ligand field theory, such enthalpic differences are expected to vary approximately as the fifth or sixth power of Δr [26]. However, other factors that influence the metal–ligand bond strength, such as the donor atom, metal ion and oxidation state, also play a role. Consequently, reactions in which the number of antibonding electrons increases only by one ($Co^{II}N_6$, $\Delta S = 1$) or for which the metal–ligand bonds are weak ($Fe^{III}S_6$) are characterized by small values of ΔH°_{se} and ΔS°_{se}. ΔH°_{se}

Table 1
Structural, thermodynamic and kinetic characteristics of spin-exchange reactions

Complex [a]	ΔH°_{se} (kJ mol^{-1})	ΔS°_{se} (J mol^{-1} K^{-1})	References	$k_{ls\rightarrow hs}$ (s^{-1})	$k_{hs\rightarrow ls}$ (s^{-1})	Method [b]	References
$Fe^{II}N_6$ ($t_{2g}^6 \rightarrow t_{2g}^4e_g^2$, $\Delta S = 2$, $\Delta r \cong 0.17$ Å)[c]							
$Fe(sar)^{2+}$	11–15	28–40	[28]				
$Fe[(6\text{-}Mepy)_2(py)tren]^{2+}$	12	36	[29]	4×10^6	5×10^6	T	[30]
$Fe[(py)imH]_3^{2+}$	15–16	49–53	[31]	1.1×10^7	1.0×10^7	T	[32]
$Fe[HB(pz)_3]_2$	16–22	48–61	[33–36]	4.9×10^6	2.5×10^7	U	[35]
$Fe(papth)_2^{2+}$	16	62	[35]	1.7×10^7	7.2×10^6	U	[35]
$Fe(2\text{-}amp)_3^{2+}$	18–25	52–88	[37]				
$Fe[(6\text{-}Mepy)(py)_2tren]^{2+}$	19	42	[29]	4×10^5	8×10^6	T	[30]
$Fe[(py)bzimH]_3^{2+}$	20–21	78–92	[31]				
$Fe(tacn)_2^{2+}$	21–24	60–78	[36,38]				
$Fe(tpen)^{2+}$	24–30	67–74	[39]	(5.8×10^6)[d]	2.9×10^7	P	[40]
$Fe(tppn)^{2+}$	25–30	62–88	[41]	(6.4×10^6)[d]	3.2×10^7	P	[40]
$Fe^{III}N_4O_2$ ($t_{2g}^5 \rightarrow t_{2g}^3e_g^2$, $\Delta S = 2$, $\Delta r \cong 0.13$ Å)							
$Fe[(acac)_2trien]^+$	7–17	44–63	[42,43]	1.6×10^8	3.2×10^8	U	[43]
$Fe(Salmeen)_2^+$	12–16	43–61	[44]				
$Fe[(Sal)_2trien]^+$	16–21	56–69	[43,45]	6.1×10^7	1.3×10^8	U	[43]
$Fe^{III}S_6$ ($t_{2g}^5 \rightarrow t_{2g}^3e_g^2$, $\Delta S = 2$, $\Delta r \cong 0.13$ Å)							
$Fe(n\text{-}Pr_2dtc)_3$	6–8	17–23	[46]	$>10^9$	$>10^9$	U	[35]
$Co^{II}N_6$ ($t_{2g}^6e_g^1 \rightarrow t_{2g}^5e_g^2$, $\Delta S = 1$, $\Delta r \cong 0.06$ Å)							
$Co(terpy)_2^{2+}$	9–16	26–55	[47]				
$Co[py(imine)_2]_2^{2+}$	11–17	30–45	[47,48]				
$Co^{III}O_6$ ($t_{2g}^6 \rightarrow t_{2g}^4e_g^2$, $\Delta S = 2$, $\Delta r \cong 0.2$ Å)							
$Co[CpCo(PO(OEt)_2)_3]_2^+$	22–26	62–76	[49–51]				

[a] Ligand abbreviations: sar = 3, 6, 10, 13, 16, 19-hexaazatricyclo [6.6.6] eicosane (sarcophagine); $(6\text{-}Mepy)_2(py)tren$ and $(6\text{-}Mepy)(py)_2tren$ = tris [4-[(6-R)-2-pyridyl]-3-aza-3-butenyl] amine, R = H or CH_3; pyimH = 2-(2′-pyridyl) imidazole; $HB(pz)_3^-$ = hydro tris (pyrazol-1-yl) borate; papth = 2-(2-pyridylamino)-4-(2-pyridyl) thiazole; 2-amp = 2-aminomethylpyridine; pybzimH = 2-(2′-pyridyl) benzimidazole; tacn = 1, 4, 7-triazacyclononane; tpen = tetrakis (2-pyridylmethyl)-1,2-ethanediamine; tppm = tetrakis (2-pyridylmethyl)-1,2-propanediamine; $(acac)_2trien^{2-}$ = hexadentate Schiff base ligand from acetylacetone (Hacac) and triethylenetetramine (trien); $Salmeen^-$ = tridentate Schiff base ligand from salicylaldehyde (Hsal) and N-methylethylenediamine (meen) $(Sal)_2trien^{2-}$ = hexadentate Schiff base ligand from salicylaldehyde (Hsal) and triethylenetetramine (trien); $n\text{-}Pr_2dtc^-$ = di(*n*-propyl) dithiocarbamate; terpy = 2,2′,2″-terpyridine; $py(imine)_2$ = N-R-2,6-pyridinedicarboxaldimine, R = $NH(CH_3)$; $CpCo(PO(OEt)_2)_3^-$ = cyclopentadienyltris (diethylphosphito-P) cobaltate.

[b] Kinetic data obtained from temperature-jump (T), ultrasonic absorption (U) or photoperturbation (P) methods.

[c] Estimated bond distance changes taken from Ref. [25] except value for $Co^{III}O_6$ from Ref. [49].

[d] Calculated from $k_{hs\rightarrow ls}$ and $K_{se} = 0.2$.

and ΔS°_{se} are larger for most spin-equilibria with $\Delta S = 2$. Even so, relatively large ligand dependences are observed, as found for $Fe^{II}N_6$ and $Fe^{III}N_4O_2$ spin transitions. As a result, ΔH°_{se} values in Table 1 span a considerable range of 6–30 kJ mol^{-1}.

The entropic differences in Table 1 arise primarily from the differences in vibrational and electronic properties of the two spin-states [52]. The vibrational partition functions increase as the metal–ligand bonds are weakened, and the electronic partition functions increase with increasing multiplicity. These changes result in a positive value of ΔS°_{se} for ls → hs conversion. The basis of this observation is analogous to that underlying the contribution of intramolecular factors to the entropies of electrochemical half-reactions [38,53,54]. Following the same approach we estimate ΔS°_{se} as $\Delta S^{\circ}_{vib} + \Delta S^{\circ}_{el}$, where $\Delta S^{\circ}_{vib} = S^{\circ}_{vib,hs} - S^{\circ}_{vib,ls}$ and $\Delta S^{\circ}_{el} = S^{\circ}_{el,hs} - S^{\circ}_{el,ls}$, and calculate these terms by the use of the following expressions:

$$S^{\circ}_{vib} = R\sum[u(e^{u} - 1)^{-1} - \ln(1 - e^{-u})] \quad (3)$$

$$S^{\circ}_{el} = R \ln q_{el} + RT\partial(\ln q_{el})/\partial T \quad (4)$$

In Eqs. (3) and (4), u equals $1.439\omega/T$, ω is the vibrational frequency in cm^{-1} and q_{el} is the electronic partition function.

The vibrational modes most affected by a change in spin-state are the metal–ligand stretching and bending frequencies. Thus, ΔS°_{vib} can be obtained to a first approximation from frequency shifts in the 15 modes associated with an ML_6 center. Unfortunately, there are no complete data for ls and hs isomers in this region. The most extensive studies are those of Hutchinson et al. [55,56], who determined from isotope substitution and temperature dependent measurements that Fe–N bands at 434 and 400 cm^{-1} in ls-Fe[HB(pz)$_3$]$_2$ shift to 258 and 223 cm^{-1} in hs-Fe[HB(pz)$_3$]$_2$. If the symmetries of both the vibrations are assumed to be E_u for these D_{3d} complexes, a value of $\Delta S^{\circ}_{vib} = 15$ J mol^{-1} K^{-1} is calculated by use of Eq. (3). However, this result includes contributions from only four of 15 possible modes. A more accurate estimate is obtained by using hexaammine complexes as a model and calculating the difference in vibrational entropy between ls-Fe$(NH_3)_6^{3+}$ (t_{2g}^5) and hs-Fe$(NH_3)_6^{2+}$ ($t_{2g}^4e_g^2$), assuming that the vibrational entropy difference between ls-Fe$(NH_3)_6^{3+}$ (t_{2g}^5) and ls-Fe$(NH_3)_6^{2+}$ (t_{2g}^6) is small because there is no change in the number of antibonding electrons. Using experimental data [57,58] and Badger's rule, we have estimated [36,38] the octahedral (A_{1g}, E_g, T_{1u}, T_{1u}, T_{2g}, T_{2u}) Fe–N frequencies of ls-Fe$(NH_3)_6^{3+}$ and hs-Fe$(NH_3)_6^{2+}$ to be 509, 363, 466, 252, 252 and 177 cm^{-1}, and 344, 245, 315, 170, 170 and 120 cm^{-1}, respectively. Application of Eq. (3) yields $\Delta S^{\circ}_{vib} = 43$ J mol^{-1} K^{-1}, which is a significant fraction of typical ΔS°_{se} values for $Fe^{II}N_6$ spin-equilibra (Table 1).

Electronic terms also contribute to ΔS°_{se}. For complexes with an A or E ground state, the electronic partition function equals the product of the spin multiplicity and the orbital degeneracy. Thus, $q_{el} = 1$ for ls-Fe$(NH_3)_6^{2+}$ ($^1A_1$). However, for hs-Fe$(NH_3)_6^{2+}$ ($^5T_2$), spin–orbit coupling allows higher-lying states to be occupied,

which decreases the total degeneracy. If it is assumed that $q_{el} = \Sigma g_i e^{-1.439\varepsilon_i/T}$ with $g_0 = 3$, $g_1 = 5$, $g_2 = 7$, $\varepsilon_1 = 163\ cm^{-1}$ and $\varepsilon_2 = 408\ cm^{-1}$, a value of $\Delta S^\circ_{el} = 20\ J\,mol^{-1}\,K^{-1}$ is calculated from Eq. (4) at 298 K [38]. Thus, the electronic contribution equals about one-half the vibrational term, and the sum of the estimated entropies ($63\ J\,mol^{-1}\,K^{-1}$) is in good accord with ΔS°_{se} for $Fe(tacn)_2^{2+}$ spin-exchange. As for ΔH°_{se}, the structural and compositional differences lead to a considerable range of ΔS°_{se} values in Table 1. However, in all cases there is a compensation of enthalpic and entropic driving force contributions, as must be the case for spin-equilibrium to be observed (i.e. $K_{se} \cong 1$).

2.2. Kinetics

The kinetics of spin-exchange reactions are also influenced by nuclear reorganization. However, because the processes are intramolecular in nature, they are invariably rapid. Table 1 contains data that have been obtained in solution by laser temperature-jump, ultrasonic absorption and photoperturbation techniques. Rate constants range approximately from 10^6 to $10^9\ s^{-1}$. In general, faster rates are observed for systems characterized by smaller structural change or weaker metal–ligand bonds; slower rates are observed for structurally more demanding transformations. Thus, there is an approximate inverse correlation between the magnitudes of the spin-exchange rate constants and the thermodynamic parameters in Table 1. Electronic factors do not present a major limitation to spin-exchange. Even for spin-forbidden $\Delta S = 2$ transitions, it is estimated that second-order coupling with the intermediate electronic state is efficient and that the electronic prefactor is not less than $\sim 10^{-2}$ [23]. As a result, spin-state isomerizations in which the immediate coordination environment of a metal ion remains intact are rapid. A comparison of electrochemical diffusion-layer and chemical reaction-layer thicknesses [59,60] reveals that voltammetric sweep rates of 10^4 to $10^7\ V\ s^{-1}$ are required to detect chemical intermediates that interconvert with first-order rates constants of 10^6–$10^9\ s^{-1}$. Although achievable [61], sweep rates of this magnitude are not commonly employed. Therefore, it is likely that spin-exchange reactions remain in equilibrium relative to electrochemical events under most conditions. The following derivations are based on this assumption.

3. Thermodynamics of coupled electron-transfer and spin-exchange reactions

3.1. Oxidation–reduction potentials

An appropriate framework for interpreting the thermodynamics of coupled electron-transfer and spin-exchange is the electrochemical square scheme shown in Scheme 1 [62–65]. Schemes of this nature describe the influence of coupled chemical reactions (proton transfer, ligand substitution, conformational change) on electron-transfer behavior and occur widely in chemical and biological systems [66–71]. Here, steps A and D are electrochemical reactions pertaining to the low- and

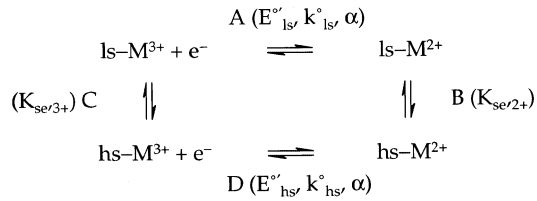

Scheme 1.

high-spin forms of an $M^{3+/2+}$ couple and have potentials $E^{\circ\prime}_{ls}$ and $E^{\circ\prime}_{hs}$, respectively. Steps B and C are the low- to high-spin conversions in each oxidation state and have equilibrium constants $K_{se,2+}$ and $K_{se,3+}$. Typically, $K_{se,2+} > K_{se,3+}$ and $E^{\circ\prime}_{hs} > E^{\circ\prime}_{ls}$, because the higher oxidation state usually exhibits a larger ligand field strength. The electrode potentials and spin-equilibrium constants are related by

$$E^{\circ\prime}_{hs} - E^{\circ\prime}_{ls} = (RT/F)\ln(K_{se,2+}/K_{se,3+}) \quad (5)$$

Determination of all the four parameters is usually impossible, because of the position of the spin-state equilibrium in either or both the oxidation states.

If all the reactions in Scheme 1 are in equilibrium, the observed potential of an $M^{3+/2+}$ couple is defined by either of the following expressions:

$$E^{\circ\prime}_{obs} = E^{\circ\prime}_{ls} + (RT/F)\ln[(1 + K_{se,2+})/(1 + K_{se,3+})] \quad (6a)$$

$$E^{\circ\prime}_{obs} = E^{\circ\prime}_{hs} + (RT/F)\ln[K_{se,3+}(1 + K_{se,2+})/K_{se,2+}(1 + K_{se,3+})] \quad (6b)$$

Because spin-exchange often is evident in only one oxidation state, Eqs. (6a) and (6b) are frequently simplified to correspond to this observation. Thus, if spin-crossover occurs in the lower oxidation state, M^{3+} is predominantly low-spin and:

$$E^{\circ\prime}_{obs} \cong E^{\circ\prime}_{ls} + (RT/F)\ln(1 + K_{se,2+}) = E^{\circ\prime}_{ls} - (RT/F)\ln(x_{ls,2+}) \quad (7)$$

If spin-crossover occurs in the higher oxidation state, M^{2+} is predominantly high-spin and:

$$E^{\circ\prime}_{obs} \cong E^{\circ\prime}_{hs} + (RT/F)\ln[K_{se,3+}/(1 + K_{se,3+})] = E^{\circ\prime}_{hs} + (RT/F)\ln(x_{hs,3+}) \quad (8)$$

In Eqs. (7) and (8), $x_{ls,2+}$ and $x_{hs,3+}$ are the mole fractions of the ls and hs species in the indicated oxidation states.

Eqs. (7) and (8) have been used to investigate the relationships between the electrode potential and the spin-state distribution. If the spin-state distribution is altered by changing the ligand substituents, its effect on $E^{\circ\prime}_{obs}$ is small. Thus, Chant et al. [72] examined a series of substituted iron tris(dithiocarbamate) complexes that exhibit a low- to high-spin-equilibrium in the Fe(III) state and undergo reduction to hs-Fe(II) and oxidation to ls-Fe(IV) species. No simple relationship between $E^{\circ\prime}_{obs}$ and the magnetic properties was found. Kadish et al. [73,74] studied the reduction of the substituted $Fe(X\text{–}Salmeen)_2^+$ and $Fe[(X\text{–}Sal)_2trien]^+$ complexes in Table 1 and observed, in contradistinction to Eq. (8), that $E^{\circ\prime}_{obs}$ becomes more negative as the proportion of hs-Fe^{3+} increases. In both cases it appears that, because the

spin-state distribution covers only a small range, its influence on $E^{\circ\prime}_{obs}$ is small and is overshadowed by the ligand substituent effects.

Larger influences on $E^{\circ\prime}_{obs}$ are observed when the spin-state distribution is altered by a change in structure or composition. For example, in the catalytic cycle of cytochrome P450, binding of the substrate (*d*-camphor) converts the active site from low-spin, six-coordinate Fe(III) to high-spin, five-coordinate Fe(III) and shifts the $Fe^{III/II}$ redox potential in the positive direction by 130 mV. Sligar and Fisher [75] measured the potentials and Fe(III) spin-equilibrium constants for the reaction using a series of substrate analogs that caused $K_{se,3+}$ to change by several orders of magnitude. $E^{\circ\prime}_{obs}$ changes in the direction predicted by Eq. (8), although the magnitude of the response is approximately twice the anticipated value.

Cobalt(III/II) hexaamine couples provide another example of the joint influence of compositional change and the spin-state distribution on $E^{\circ\prime}_{obs}$. These spin-state equilbria are displaced largely towards the low-spin form as CoN_6^{3+} ($K_{se,3+} \ll 1$) and towards the high-spin form as CoN_6^{2+} ($K_{se,2+} \gg 1$). Thus, there is presumed to be a large difference between the potentials of the pure ls and pure hs half-reactions, although these parameters have not been measured. The potentials of ls-CoN_6^{3+}/hs-CoN_6^{2+} couples extend approximately from $+0.3$ to -0.6 V vs NHE [13]. This property has been investigated through various modeling studies [76–78], from which it is evident that the energetics of the spin-equilibrium steps make a large contribution to the variation in $E^{\circ\prime}_{obs}$ with ligand structure.

3.2. Half-reaction entropies

A useful quantity in understanding coupled electron-transfer and spin-exchange is the electrochemical half-reaction entropy, ΔS°_{rc}. This parameter equals the difference in entropy between the reduced and oxidized forms of a redox couple:

$$\Delta S^{\circ}_{rc} = S^{\circ}_{red} - S^{\circ}_{ox} = F(\partial E^{\circ\prime}/\partial T) \tag{9}$$

It is determined from the temperature dependence of the $Ox + e^- = Red$ potential measured in a non-isothermal electrochemical cell (i.e. one in which the temperature of the indicating electrode is varied and the temperature of the reference electrode is held constant) [79]. When a spin-exchange and an electron-transfer occur concurrently, the observed half-reaction entropy is given by the temperature derivative of Eq. (6a) or Eq. (6b):

$$(\Delta S^{\circ}_{rc})_{obs} = (\Delta S^{\circ}_{rc})_{ls} + x_{hs,2+}\Delta S^{\circ}_{se,2+} - x_{hs,3+}\Delta S^{\circ}_{se,3+} + \Delta S^{\circ}_{mix} \tag{10a}$$

$$(\Delta S^{\circ}_{rc})_{obs} = (\Delta S^{\circ}_{rc})_{hs} + x_{ls,3+}\Delta S^{\circ}_{se,3+} - x_{ls,2+}\Delta S^{\circ}_{se,3+} + \Delta S^{\circ}_{mix} \tag{10b}$$

where $\Delta S^{\circ}_{mix} = R(x_{hs,3+} \ln x_{hs,3+} + x_{ls,3+} \ln x_{ls,3+} - x_{hs,2+} \ln x_{hs,2+} - x_{ls,2+} \ln x_{ls,2+})$.

The impact of the spin-state equilibria on the electrochemical half-reaction entropies is illustrated by the $Fe(tacn)_2^{3+/2+}$ couple. The Fe(III) complex is low-spin and is reduced to a ls–hs mixture of $Fe(tacn)_2^{2+}$.

$$\text{ls}-\text{Fe(tacn)}_2^{3+} + \text{e}^- \rightleftharpoons \text{ls}-\text{Fe(tacn)}_2^{2+} \quad E^{\circ\prime}_{\text{ls}} \tag{11}$$

$$\text{ls}-\text{Fe(tacn)}_2^{2+} \rightleftharpoons \text{hs}-\text{Fe(tacn)}_2^{2+} \quad K_{\text{se},2+} \tag{12}$$

The magnitude of $K_{\text{se},2+}$ is such that Fe(II) is ca. 25% high-spin at room temperature. Observation of an unusually large value of $\Delta S^\circ_{\text{rc}}$ for $\text{Fe(tacn)}_2^{3+/2+}$ led us to suspect the presence of the Fe(II) spin-state equilibrium, which we subsequently confirmed by magnetic and spectroscopic measurements [36,38,80]. Fig. 1 shows a plot of $E^{\circ\prime}_{\text{obs}}$ vs T for $\text{Fe(tacn)}_2^{3+/2+}$ in dimethyl sulfoxide containing 0.1 M $LiClO_4$. The apparent half-reaction entropy of 138 J mol^{-1} K^{-1} is larger than the value observed for comparable $M^{3+/2+}$ couples without a spin-state change in this solvent. A value of $\Delta S^\circ_{\text{rc}}$ for the low-spin $\text{Fe(tacn)}_2^{3+/2+}$ couple is obtained by expressing $E^{\circ\prime}_{\text{ls}}$ as $E^{\circ\prime}_{\text{obs}} - (RT/F)\ln(1 + K_{\text{se},2+})$ and using values of $\Delta H^\circ_{\text{se},2+} = 22.4$ kJ mol^{-1} and $\Delta S^\circ_{\text{se},2+} = 68.4$ J mol^{-1} K^{-1} to calculate $E^{\circ\prime}_{\text{ls}}$ at each temperature. The resultant plot of $E^{\circ\prime}_{\text{ls}}$ vs T is shown in Fig. 1, from which a value of $\Delta S^\circ_{\text{rc}} = 103$ J mol^{-1} K^{-1} is obtained for the reduction of ls-Fe(tacn)_2^{3+} to ls-Fe(tacn)_2^{2+}. This corrected result is nearly identical to $\Delta S^\circ_{\text{rc}}$ for $\text{Ru(tacn)}_2^{3+/2+}$ under the same experimental conditions (110 J mol^{-1} K^{-1}) [36]. The Ru(III/II) couple is a good calibrant for pure low-spin behavior, because it undergoes ls/ls reduction and experiences little inner-shell reorganization.

Eqs. (10a) and (10b) are also applicable to half-reactions in which the spin-state distribution is altered by a change in ligand substituent. A necessary assumption is that $\Delta S^\circ_{\text{rc}}$ for the pure ls–ls and hs–hs couples and $\Delta S^\circ_{\text{se}}$ for the individual oxidation states are independent of this structural variation. In this vein, Kadish [73,74] measured the entropies for the $[\text{Fe(X–Sal)}_2\text{trien}]^{+/0}$ and $[\text{Fe(X–Salmeen)}_2]^{+/0}$ half-reactions in which the position of the Fe(III) spin-state equilibrium was changed by varying X. If $\Delta S^\circ_{\text{mix}}$ is ignored, Eq. (10a) reduces to $(\Delta S^\circ_{\text{rc}})_{\text{obs}} =$

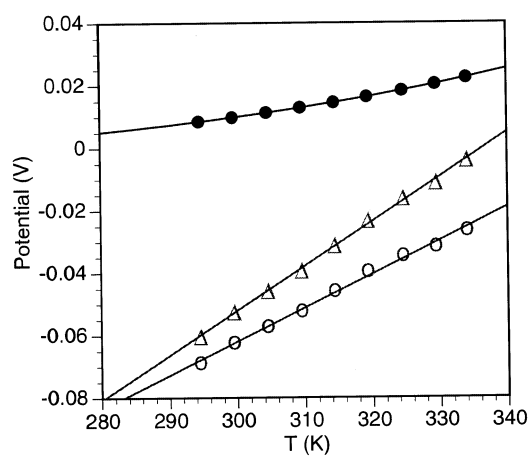

Fig. 1. Plots of $E^{\circ\prime}_{\text{obs}}$ (△), $E^{\circ\prime}_{\text{obs}} - (RT/F)\ln(1 + K_{\text{se},2+})$ (○) and $(RT/F)\ln(1 + K_{\text{se},2+})$ (●) vs temperature for the reduction of Fe(tacn)_2^{3+} in dimethylsulfoxide containing 0.1 M $LiClO_4$; from data in Ref. [36].

$(\Delta S^{\circ}_{rc})_{ls} + \Delta S^{\circ}_{se,2+} - x_{hs,3+}\Delta S^{\circ}_{se,3+}$. Fig. 2 displays a plot of $(\Delta S^{\circ}_{rc})_{obs}$ vs $x_{hs,3+}$ for the $[Fe(X\text{–}Sal)_2trien]^{+/0}$ couple. The slope of the line equals 66 J mol^{-1} K^{-1}, a result that is consistent with the range of $\Delta S^{\circ}_{se,3+}$ values exhibited by the $[Fe(X\text{–}Sal)_2trien]^{+}$ complexes in Table 1. The magnitude of $(\Delta S^{\circ}_{rc})_{obs}$ at $x_{hs,3+} = 1$ equals the half-reaction entropy of the hs-$[Fe(X\text{–}Sal)_2trien]^{+/0}$ couple (58 J mol^{-1} K^{-1}), whereas that at $x_{hs,3+} = 0$ (124 J mol^{-1} K^{-1}) equals $(\Delta S^{\circ}_{rc})_{ls} + \Delta S^{\circ}_{se,2+}$. With suitable calibrants, it may be possible to estimate unknown quantities such as $\Delta S^{\circ}_{se,2+}$ in this way.

4. Kinetics of coupled electron-transfer and spin-exchange reactions

4.1. Electrochemical rate constants

The kinetics of coupled electrochemical and spin-exchange reactions are also interpreted in terms of Scheme 1. It is assumed that the spin-exchange reactions are in equilibrium and that the electron-transfer does not occur across the diagonal paths connecting the low- and high-spin forms. The observed electrochemical rate constant, k°_{obs}, is expressed as the sum of the two terms described by Butler–Volmer theory [59]:

$$k^{\circ}_{obs} = (k^{\circ}_{obs})_{ls} + (k^{\circ}_{obs})_{hs} \tag{13}$$

$(k^{\circ}_{obs})_{ls}$ is the rate constant for the reduction of M^{3+} to M^{2+} by reactions A plus B and is termed the *low-spin pathway*:

$$(k^{\circ}_{obs})_{ls} = (x_{ls,2+})^{\alpha}(x_{ls,3+})^{1-\alpha}k^{\circ}_{ls} \tag{14}$$

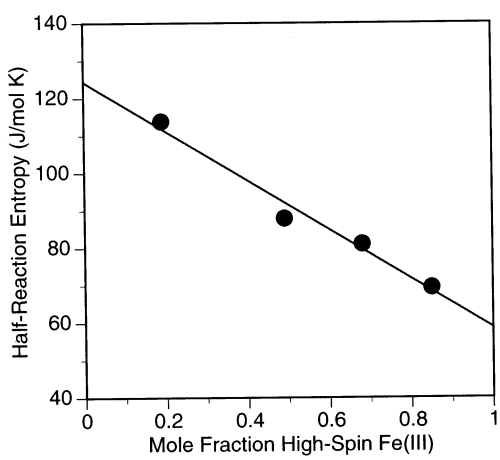

Fig. 2. Plot of observed half-reaction entropy vs mole fraction of high-spin Fe(III) for $[Fe(Sal)_2trien]^{+/0}$ redox couples; from data in Ref. [73].

Table 2
Heterogeneous electron-transfer rate constants and spin-equilibrium data for $[Fe(X–Salmeen)_2]^{+/0}$ and $[Fe(X–Sal)_2trien]^{+/0}$ couples[a]

X	k°_{obs} (cm s^{-1}) [b]	$K_{se,3+}$ [c]	$x_{hs,3+}$ [c]
$[Fe(X–Salmeen)_2]^{+/0}$			
3-OCH_3	0.060	3.6	0.78
4-OCH_3	0.059	2.5	0.71
H	0.046	1.0	0.5
3-NO_3	0.030	0.71	0.42
5-NO_3	0.020	0.37	0.27
$[Fe(X–Sal)_2trien]^{+/0}$			
5-OCH_3	0.047	5.7	0.85
3-OCH_3	0.040	2.7	0.73
H	0.033	1.4	0.58
3-NO_3	0.028	0.96	0.49
5-NO_3	0.024	0.23	0.19

[a] From Refs. [74,82].
[b] Measured in acetone containing 0.1 M tetraethyl-ammonium perchlorate.
[c] Measured in acetone without supporting electrolyte.

$(k^\circ_{obs})_{hs}$ is the rate constant for the reduction of M^{3+} to M^{2+} by reactions C plus D and is termed the *high-spin pathway*:

$$(k^\circ_{obs})_{hs} = (x_{hs,2+})^{\alpha}(x_{hs,3+})^{1-\alpha}k^\circ_{hs} \quad (15)$$

In the above equations k°_{ls} and k°_{hs} are the intrinsic electrochemical rate constants of the low- and high-spin half-reactions, α is the electrochemical transfer coefficient (assumed equal to 0.5 in all cases), and $x_{ls,i} = 1/(1 + K_{se,i})$ and $x_{hs,i} = K_{se,i}/(1 + K_{se,i})$ are the mole fractions of the low- and high-spin forms in the indicated oxidation state.

It is generally regarded that electron-transfer reactions accompanied by a change in spin-state are slower than those that are not. Intuitively, this is anticipated because large nuclear reorganizations accompany spin-crossover. However, if spin-exchange is rapid in comparison with thermal electron-transfer, its reorganizational barriers will not limit the overall reaction rate. Rather, as shown by Eqs. (13)–(15), changes in the equilibrium distribution of electroactive species will influence k°_{obs}. Several investigations have demonstrated this expectation on a qualitative to semi-quantitative basis. Aoyagui and co-workers [81] examined a series of $Fe(R_2dtc)_3^{+/0}$ and $Fe(R_2dtc)_3^{0/-}$ couples and found that the half-reactions characterized by Fe(III) spin-equilibria were slower than those that lacked this feature. Kadish and co-workers [74,82] correlated k°_{obs} with the position of low- to high-spin-equilibrium by varying the substituent in $[Fe(X–Salmeen)_2]^{+/0}$ and $[Fe(X–Sal)_2trien]^{+/0}$ couples. These half-reactions are assumed to follow the high-spin pathway, because spin-equilibrium occurs in the Fe(III) state and $x_{ls,2+} \approx 0$. In accord with this expectation, the data in Table 2 show that k°_{obs} increases systemat-

ically with $x_{hs,3+}$. However, the range of k°_{obs} values is small, and k°_{obs} varies linearly with the mole fraction rather than its square root as predicted by Eq. (15). Other investigations found no correlation between the electrochemically measured rate constants and the spin-state distributions for $Fe[(6\text{-}Mepy)_n(py)_{3-n}tren]^{3+/2+}$ [83], $Co[py(imine)_2]_2^{3+/2+}$ [84] and $Fe^{III/II}$-porphyrin couples [85]. As is true for electrode potentials (Section 3.1), it appears that the spin-state distributions displaced over a small range of values have a correspondingly small impact on the electron-transfer rate constants.

4.2. Electrochemical activation parameters

A more effective means of diagnosing coupled electron-transfer and spin-exchange reactions is provided by the electrochemical activation parameters $\Delta H^{\ddagger}_{obs}$ and $\Delta S^{\ddagger}_{obs}$. These terms are obtained from the temperature dependence of k°_{obs} measured in a non-isothermal electrochemical cell [86]:

$$k^{\circ}_{obs} = A \exp[\Delta S^{\ddagger}_{obs}/R] \exp[-\Delta H^{\ddagger}_{obs}/RT] \quad (16)$$

$$\Delta H^{\ddagger}_{obs} = -R\, \partial[\ln(k^{\circ}_{obs})]/\partial(1/T) \quad (17)$$

$$\Delta S^{\ddagger}_{obs} = R \ln[(k^{\circ}_{obs})/A] + \Delta H^{\ddagger}_{obs}/T \quad (18)$$

For electrochemical reactions it is anticipated that $\Delta S^{\ddagger}_{obs} = 0$ and $\Delta H^{\ddagger}_{obs} = \Delta H^{\ddagger}_{is} + \Delta H^{\ddagger}_{os}$, where $\Delta H^{\ddagger}_{is}$ and $\Delta H^{\ddagger}_{os}$ are the inner- and outer-shell reorganization enthalpies calculated using simple harmonic oscillator and dielectric continuum models [87,88], respectively. A is the electrochemical prefactor and is assigned a value of 2×10^3 cm s^{-1}. Although this value is smaller than the quantity $\sim 5 \times 10^4$ cm s^{-1} commonly employed in the encounter pre-equilibrium model of electrochemical kinetics [89], it is close to the value predicted by the collisional model of heterogeneous electron-transfer ($A = (kT/2\pi m)^{1/2}$, m = mol wt) [90] and is consistent with the experimentally determined prefactors of transition metal redox couples in aqueous solution [91].

Table 3 summarizes the data for $M(tacn)_2^{3+/2+}$ couples [27] that illustrate the influence of the coupled spin-exchange on electrochemical activation parameters.

Table 3
Electrochemical activation parameters for $M(tacn)_2^{3+/2+}$ couples[a]

Couple	k°_{obs} (cm s^{-1})	$\Delta S^{\ddagger}_{obs}$ (J mol^{-1} K^{-1})	$\Delta H^{\ddagger}_{obs}$ (kJ mol^{-1})	$\Delta H^{\ddagger}_{calc}$[b] (kJ mol^{-1})
$Ru(tacn)_2^{3+/2+}$	1.3	−7	16	15
$Ni(tacn)_2^{3+/2+}$	0.12	−4	23	24
$Co(tacn)_2^{3+/2+}$	0.016	137	70	40
$Fe(tacn)_2^{3+/2+}$	2.5	35	27	16

[a] Obtained in aqueous NaF solution and corrected for electrical double layer effects as described in Ref. [27].

[b] $\Delta H^{\ddagger}_{calc} = \Delta H^{\ddagger}_{is} + \Delta H^{\ddagger}_{os}$ calculated by use of simple harmoic oscillator and dielectric continuum models.

All four examples exhibit k°_{obs} values that decrease as the calculated barrier height increases and, thus, are congruent with the Marcus theory [92]. Moreover, Ru(tacn)$_2^{3+/2}$ and Ni(tacn)$_2^{3+/2}$, which undergo electron-transfer without an accompanying change in spin-state, exhibit $\Delta S^{\ddagger}_{obs}$ near zero and experimental activation enthalpies in agreement with the calculated $\Delta H^{\ddagger}_{is} + \Delta H^{\ddagger}_{os}$. The $\Delta H^{\ddagger}_{obs}$ value for Ni(tacn)$_2^{3+/2}$ reflects a contribution from inner-shell reorganization that arises from the difference in number of antibonding electrons between Ni^{3+} ($t_{2g}^6 e_g^1$) and Ni^{2+} ($t_{2g}^6 e_g^2$). However, the cobalt and iron couples, which are characterized by complete or partial spin-exchange in conjunction with electron-transfer, display $\Delta H^{\ddagger}_{obs}$ and $\Delta S^{\ddagger}_{obs}$ values that are much larger than predicted, even after considering the inner-shell contributions to the barrier height. For Co(tacn)$_2^{3+/2}$, the conversion from to low- to high-spin is complete upon reduction; for Fe(tacn)$_2^{3+/2}$, the spin-state distribution of Fe(II) is ca. 25% hs/75% ls at room temperature.

To understand the origins of these observations, we have examined the temperature dependence of the apparent electrochemical rate constants described by Scheme 1. The activation parameters observed are obtained from the inverse temperature derivatives of the logarithmic forms of Eqs. (14) and (15). Thus, for reactions proceeding through the low-spin pathway:

$$(\Delta H^{\ddagger}_{obs})_{ls} = \Delta H^{\ddagger}_{ls} - \alpha(x_{hs,2+})\Delta H^{\circ}_{se,2+} - (1-\alpha)(x_{hs,3+})\Delta H^{\circ}_{se,3+} \quad (19)$$

$$(\Delta S^{\ddagger}_{obs})_{ls} = \Delta S^{\ddagger}_{ls} - \alpha(x_{hs,2+})\Delta S^{\circ}_{se,2+} - (1-\alpha)(x_{hs,3+})\Delta S^{\circ}_{se,3+} + \alpha R \ln(x_{hs,2+}) + (1-\alpha)R \ln(x_{hs,3+}) \quad (20)$$

For reactions proceeding through the high-spin pathway:

$$(\Delta H^{\ddagger}_{obs})_{hs} = \Delta H^{\ddagger}_{hs} + \alpha(x_{ls,2+})\Delta H^{\circ}_{se,2+} + (1-\alpha)(x_{ls,3+})\Delta H^{\circ}_{se,3+} \quad (21)$$

$$(\Delta S^{\ddagger}_{obs})_{hs} = \Delta S^{\ddagger}_{hs} + \alpha(x_{ls,2+})\Delta S^{\circ}_{se,2+} + (1-\alpha)(x_{ls,3+})\Delta S^{\circ}_{se,3+} + \alpha R \ln(x_{hs,2+}) + (1-\alpha)R \ln(x_{hs,3+}) \quad (22)$$

In Eqs. (19)–(22) $\Delta H^{\ddagger}_{ls}$, $\Delta S^{\ddagger}_{ls}$, $\Delta H^{\ddagger}_{hs}$ and $\Delta S^{\ddagger}_{hs}$ are the activation parameters for the unperturbed ls/ls and hs/hs electron-transfer reactions. In general, we anticipate that $\Delta S^{\ddagger}_{ls}$ and $\Delta S^{\ddagger}_{hs} \approx 0$ and that $\Delta H^{\ddagger}_{ls}$ and $\Delta H^{\ddagger}_{hs}$ can be estimated from the Marcus theory or by comparison with suitable analog systems. An important finding of the above derivation is that the magnitudes of $\Delta H^{\ddagger}_{obs}$ and $\Delta S^{\ddagger}_{obs}$ reflect the mechanistic pathway of the coupled electron-transfer and spin-exchange. Thus, $\Delta H^{\ddagger}_{obs}$ and $\Delta S^{\ddagger}_{obs}$ *increase* for reactions proceeding through the *hs* pathway and *decrease* for reactions proceeding through the *ls* pathway. This result is consistent with the consequences of a temperature change on the rates of the coupled electrochemical and spin-exchange reactions described in Scheme 1. A decrease in temperature (increase in $1/T$) shifts both the spin-state equilibria towards the low-spin forms, which inhibits the electron-transfer through the high-spin pathway and increases the apparent activation enthalpy of the reactions proceeding by this route. The converse happens for the electron-transfer through the low-spin path. Also, it is possible for the electron-transfer to proceed through the high- and low-spin pathways simultaneously, in which case a partial or complete cancellation of

Table 4
Electrochemical rate constants, activation parameters and Fe(II) spin-equilibrium data for iron–poly(pyrazolyl)borate couples[a,b]

Couple	Spin-state	$K_{se,2+}$[c]	$k°_{obs}$ (cm s^{-1})	$\Delta H^{\ddagger}_{obs}$ (kJ mol^{-1})	$\Delta S^{\ddagger}_{obs}$ (J mol^{-1} K^{-1})
$Fe[B(pz)_4]_2^{+/0}$	ls–ls	$\ll 1$	1.5	20	7
$Fe[HB(pz)_3]_2^{+/0}$	ls–(ls–hs)	0.20	2.2	15	−5
$Fe[HB(Me_2pz)_3]_2^{+/0}$	ls–hs	$\gg 1$	0.088	26	7

[a] Ligand abbreviations: $B(pz)_4^-$ = tetrakis(pyrazol-1-yl)borate; $HB(pz)_3^-$ = hydrotris(pyrazol-1-yl)-borate; $HB(Me_2pz)_3^-$ = hydrotris(3,5-dimethylpyrazol-1-yl)borate.

[b] Determined in acetone/tetrahydrofuran (THF) containing 0.3 M tetrabutyl-ammonium hexafluorophosphate as described in Ref. [36].

[c] Determined from temperature dependent magnetic susceptibility measurements in d_6-THF.

spin-equilibrium contributions to $\Delta H^{\ddagger}_{obs}$ and $\Delta S^{\ddagger}_{obs}$ would occur. However, the data in Table 3 indicate that the $Co(tacn)_2^{3+/2}$ and $Fe(tacn)_2^{3+/2}$ half-reactions favor the high-spin pathway. For $Fe(tacn)_2^{3+/2}$, this occurs although the hs form is the minor isomer in both the oxidation states. For $Co(tacn)_2^{3+/2}$, this requires participation of an unfavorable Co(III) spin-state that is characterized by large thermodynamic parameters ($\Delta H°_{se,3+}$ and $\Delta S°_{se,3+}$). However, the activation parameters suggest that the minor spin-state populations are kinetically significant in these $Fe^{3+/2+}$ and $Co^{3+/2+}$ electron-transfers. To further explore these observations, we examined [36] the behavior of a series of $Fe^{III/II}$-poly(pyrazolyl)borate complexes [33] in which the position of the Fe(II) spin-equilibrium is altered by changes in the ligand stucture. The results are summarized in Table 4. The $Fe[B(pz)_4]_2$ complex is low-spin, $Fe[HB(Me_2pz)_3]_2$ is high-spin and $Fe[HB(pz)_3]_2$ exhibits a spin-equilibrium with $K_{se,2+} = 0.20$. The Fe(III) states of all the three compounds are low-spin. Thus, the $Fe[B(pz)_4]_2^{+/0}$ couple is exclusively low-spin, and the $Fe[HB(pz)_3]_2^{+/0}$ and $Fe[HB(Me_2pz)_3]_2^{+/0}$ couples are characterized by partial and complete spin-exchange, respectively, in conjunction with the electron-transfer. The observed rate constants for $Fe[B(pz)_4]_2^{+/0}$ and $Fe[HB(pz)_3]_2^{+/0}$ are large and near the practical limit of electrochemical measurements; $k°_{obs}$ for $Fe[HB(Me_2pz)_3]_2^{+/0}$ is more than one order of magnitude smaller. The activation parameters of these couples differ considerably in behavior from those of $Fe(tacn)_2^{3+/2+}$. The values of $\Delta H^{\ddagger}_{obs}$ and $\Delta S^{\ddagger}_{obs}$ for $Fe[HB(pz)_3]_2^{+/0}$ are somewhat smaller than for the ls–ls $Fe[B(pz)_4]_2^{+/0}$ couple, and $\Delta H^{\ddagger}_{obs}$ is only slightly larger in the case of $Fe[HB(Me_2pz)_3]_2^{+/0}$. These results suggest that the low-spin pathway is more important for these $Fe^{3+/2+}$ couples or that there is a cancellation of the spin-state contributions to their activation parameters. An explanation for the difference in behavior between the tacn and poly(pyrazolyl)borate complexes is not apparent at this time, but further experimentation along these lines will provide a greater understanding of the mechanistic details of the coupled electron-transfer and spin-exchange.

Acknowledgements

Support of this research by the National Science Foundation (Grant No. CHE-9988694) is gratefully acknowledged.

References

[1] W.R. Scheidt, C.A. Reed, Chem. Rev. 81 (1981) 543.
[2] I. Bertini, H.B. Gray, S.J. Lippard, J.S. Valentine, Bioinorganic Chemistry, University Science Books, Sausalito, CA, 1994.
[3] S.J. Lippard, J.M. Berg, Principles of Bioinorganic Chemistry, University Science Books, Mill Valley, CA, 1994.
[4] W. Kaim, B. Schwederski, Bioinorganic Chemistry: Inorganic Elements in the Chemistry of Life, Wiley, New York, 1995.
[5] O. Kahn, C.J. Martinez, Science 279 (1998) 44.
[6] L. Fabbrizzi, M. Licchelli, P. Pallavicini, Acc. Chem. Res. 32 (1999) 846.
[7] M. Venturi, A. Credi, V. Balzani, Coord. Chem. Rev. 185–186 (1999) 233.
[8] S.G. Sligar, Biochemistry 15 (1976) 5399.
[9] E.J. Mueller, P.J. Lioda, S.G. Sligar, in: P.R. Ortiz de Montellano (Ed.), Cytochrome P450: Structure, Mechanism and Biochemistry, 2nd ed., Plenum Press, New York, 1995 (Chap. 3).
[10] D.C. Rees, M.K. Chan, J. Kim, Adv. Inorg. Chem. 40 (1993) 89.
[11] B.K. Burgess, D.J. Lowe, Chem. Rev. 96 (1996) 2983.
[12] H. Lopes, G.W. Pettigrew, I. Moura, J.J.G. Moura, J. Biol. Inorg. Chem. 3 (1998) 632.
[13] P. Hendry, A. Ludi, Adv. Inorg. Chem. 35 (1990) 117.
[14] H.C. Stynes, J.A. Ibers, Inorg. Chem. 10 (1971) 2304.
[15] E. Buhks, M. Bixon, J. Jortner, G. Navon, Inorg. Chem. 18 (1979) 2014.
[16] D.A. Geselowitz, H. Taube, Adv. Inorg. Bioinorg. Mech. 1 (1982) 391.
[17] S. Larsson, K. Ståhl, M.C. Zerner, Inorg. Chem. 25 (1986) 3033.
[18] D.A. Geselowitz, Inorg. Chim. Acta 154 (1988) 225.
[19] M.D. Newton, J. Phys. Chem. 95 (1991) 30.
[20] R.D. Shalders, T.W. Swaddle, Inorg. Chem. 34 (1995) 4815.
[21] T.W. Swaddle, Can. J. Chem. 74 (1996) 631.
[22] E. König, Progr. Inorg. Chem. 35 (1987) 527.
[23] J.K. Beattie, Adv. Inorg. Chem. 32 (1988) 1.
[24] H. Toftlund, Coord. Chem. Rev. 94 (1989) 67.
[25] E. König, Struct. Bonding 76 (1991) 51.
[26] P. Gütlich, A. Hauser, H. Spiering, in: E.I. Solomon, A.B.P. Lever (Eds.), Inorganic Electronic Structure and Spectroscopy: Applications and Case Studies, Vol. II, Wiley, New York, 1999.
[27] P.W. Crawford, F.A. Schultz, Inorg. Chem. 33 (1994) 4344.
[28] L.L. Martin, R.L. Martin, A.M. Sargeson, Polyhedron 13 (1994) 1969.
[29] M.A. Hoselton, L.J. Wilson, R.S. Drago, J. Am. Chem. Soc. 97 (1975) 1722.
[30] M.A. Hoselton, R.S. Drago, L.J. Wilson, N. Sutin, J. Am. Chem. Soc. 98 (1976) 6967.
[31] K.A. Reeder, E.V. Dose, L.J. Wilson, Inorg. Chem. 17 (1978) 1071.
[32] E.V. Dose, M.A. Hoselton, N. Sutin, M.F. Tweedle, L.J. Wilson, J. Am. Chem. Soc. 100 (1978) 1141.
[33] J.P. Jesson, S. Trofimenko, D.R. Eaton, J. Am. Chem. Soc. 89 (1967) 3158.
[34] J.K. Beattie, N. Sutin, D.H. Turner, G.W. Flynn, J. Am. Chem. Soc. 95 (1973) 2052.
[35] J.K. Beattie, R.A. Binstead, R.J. West, J. Am. Chem. Soc. 100 (1978) 3044.
[36] J.W. Turner, PhD Dissertation, Indiana University Purdue University Indianapolis, 2000.
[37] H.L. Chum, J.A. Vanin, M.I.D. Holanda, Inorg. Chem. 21 (1982) 1146.
[38] J.W. Turner, F.A. Schultz, Inorg. Chem. 38 (1999) 358.

[39] H.-R. Chang, J.K. McCusker, H. Toftlund, S.R. Wilson, A.X. Trautwein, H. Winkler, D.N. Hendrickson, J. Am. Chem. Soc. 112 (1990) 6814.
[40] J.K. McCusker, A.L. Rheingold, D.N. Hendrickson, Inorg. Chem. 35 (1996) 2100.
[41] J.J. McGarvey, I. Lawthers, K. Heremans, H. Toftlund, Inorg. Chem. 29 (1990) 252.
[42] E.V. Dose, K.M.M. Murphy, L.J. Wilson, Inorg. Chem. 15 (1976) 2622.
[43] R.A. Binstead, J.K. Beattie, T.G. Dewey, D.H. Turner, J. Am. Chem. Soc. 102 (1980) 6442.
[44] R.H. Petty, E.V. Dose, M.F. Tweedle, L.J. Wilson, Inorg. Chem. 17 (1978) 1064.
[45] M.F. Tweedle, L.J. Wilson, J. Am. Chem. Soc. 98 (1976) 4824.
[46] D.F. Evans, T.A. James, J. Chem. Soc. Dalton Trans. (1979) 723.
[47] J.K. Beattie, R.A. Binstead, M.T. Kelso, P. Del Favero, T.G. Dewey, D.H. Turner, Inorg. Chim. Acta 235 (1995) 245.
[48] M.G. Simmons, L.J. Wilson, Inorg. Chem. 16 (1977) 126.
[49] P. Gütlich, B.R. McGarvey, W. Klaüi, Inorg. Chem. 19 (1980) 3704.
[50] G. Navon, W. Klaüi, Inorg. Chem. 23 (1984) 2722.
[51] W. Klaüi, W. Eberspach, P. Gütlich, Inorg. Chem. 26 (1987) 3977.
[52] M. Sorai, S. Seki, J. Phys. Chem. Solids 35 (1974) 555.
[53] D.E. Richardson, P. Sharpe, Inorg. Chem. 30 (1991) 1412.
[54] D.E. Richardson, P. Sharpe, Inorg. Chem. 32 (1993) 1809.
[55] B. Hutchinson, M. Hoffbauer, Spectrochim. Acta A 32 (1976) 1785.
[56] F. Grandjean, G.J. Long, B.B. Hutchinson, L. Ohlhausen, P. Neill, J.D. Holcomb, Inorg. Chem. 28 (1989) 4406.
[57] K.H. Schmidt, A. Müller, Inorg. Chem. 14 (1975) 2183.
[58] B.N. Cynvin, S.J. Cynvin, K.H. Schmidt, A. Müller, J. Brunvoll, J. Mol. Struct. 32 (1976) 269.
[59] A.J. Bard, L.R. Faulkner, Electrochemical Methods: Principles and Applications, Wiley, New York, 1980.
[60] C.P. Andrieux, J.-M. Savéant, J. Electroanal. Chem. 205 (1986) 43.
[61] C. Amatore, E. Maisonhaute, G. Simonneau, J. Electroanal. Chem. 486 (2000) 141.
[62] J. Jacq, J. Electroanal. Chem. 29 (1971) 149.
[63] A.M. Bond, K.B. Oldham, J. Phys. Chem. 89 (1985) 3739.
[64] E. Laviron, L. Roullier, J. Electroanal. Chem. 186 (1985) 1.
[65] S.A. Lerke, D.H. Evans, S.W. Feldberg, J. Electroanal. Chem. 296 (1990) 299.
[66] A. Vallat, M. Person, L. Roullier, E. Laviron, Inorg. Chem. 26 (1987) 332.
[67] K. Araki, C.-F. Shu, F.C. Anson, Inorg. Chem. 30 (1991) 3043.
[68] B.S. Brunschwig, N. Sutin, J. Am. Chem. Soc. 111 (1989) 7454.
[69] H.B. Gray, J.R. Winkler, Annu. Rev. Biochem. 65 (1996) 537.
[70] V.L. Davidson, Biochemistry 39 (2000) 4924.
[71] P. Wijetunge, C.P. Kulatilleke, L.T. Dressel, M.J. Heeg, L.A. Ochrymowycz, D.B. Rorabacher, Inorg. Chem. 39 (2000) 2897.
[72] R. Chant, A.R. Hendrickson, R.L. Martin, N.M. Rohde, Inorg. Chem. 14 (1975) 1894.
[73] K.M. Kadish, K. Das, D. Schaeper, C.L. Merrill, B.R. Welch, L.J. Wilson, Inorg. Chem. 19 (1980) 2816.
[74] T. Zhu, C.-H. Su, D. Schaeper, B.K. Lemke, L.J. Wilson, K.M. Kadish, Inorg. Chem. 23 (1984) 4345.
[75] M.T. Fisher, S.G. Sligar, J. Am. Chem. Soc. 107 (1985) 5018.
[76] T.W. Hambley, Inorg. Chem. 27 (1988) 2496.
[77] P. Comba, A.F. Sickmüller, Inorg. Chem. 36 (1997) 4500.
[78] P. Comba, Coord. Chem. Rev. 182 (1999) 343.
[79] E.L. Yee, R.J. Cave, K.L. Guyer, P. Tyma, M.J. Weaver, J. Am. Chem. Soc. 101 (1979) 1131.
[80] J.W. Turner, F.A. Schultz, Inorg. Chem., submitted for publication.
[81] H. Yasuda, K. Suga, S. Aoyagui, J. Electroanal. Chem. 86 (1978) 259.
[82] K.M. Kadish, C.H. Su, L.J. Wilson, Inorg. Chem. 21 (1982) 2312.
[83] K.M. Kadish, C.-H. Su, D. Schaeper, C.L. Merrill, L.J. Wilson, Inorg. Chem. 21 (1982) 3433.
[84] T. Zhu, C.H. Su, B.K. Lemke, L.J. Wilson, K.M. Kadish, Inorg. Chem. 23 (1983) 2527.
[85] K.M. Kadish, C.H. Su, J. Am. Chem. Soc. 105 (1983) 177.

[86] M.J. Weaver, J. Phys. Chem. 80 (1976) 2645.
[87] M.J. Weaver, in: R.G. Compton (Ed.), Comprehensive Chemical Kinetics, Vol. 27, Elsevier, Amsterdam, 1987, pp. 1–60.
[88] N. Sutin, Prog. Inorg. Chem. 30 (1983) 441.
[89] J.T. Hupp, M.J. Weaver, J. Electroanal. Chem. 152 (1983) 1.
[90] R.A. Marcus, Electrochim. Acta 13 (1968) 995.
[91] J.T. Hupp, H.Y. Liu, J.K. Farmer, T. Gennett, M.J. Weaver, J. Electroanal. Chem. 168 (1984) 313.
[92] R.A. Marcus, Angew. Chem. Int. Ed. Engl. 32 (1993) 1111.